

---

## CHAPTER 5

# Methods for rapid determination of the composition and condition of nitrocellulose propellants based on thermodynamic modeling

---

Oleksandr Brunetkin  
Oksana Maksymova  
Yevhenii Dobrynin  
Oleksandr Sidelynikov

### Abstract

A method for rapid verification of the composition and energetic characteristics of nitrocellulose propellants is presented. It is based on a library approach to solving direct and inverse problems of thermal decomposition modeling. The library method forms a multidimensional array of solutions by varying elemental composition, enthalpy, and combustion conditions. This approach allows efficient determination of propellant composition from measurable parameters, primarily the temperature and combustion conditions of the reaction products, even in ill-conditioned inverse problems. An algorithm for encoding initial parameters and a procedure for successive data reduction ensure unambiguous reconstruction of the composition. Special attention is given to modeling combustion in closed volumes, selecting real-gas equations of state, accounting for pressure effects, chemical equilibrium, and possible formation of condensed phases. The results provide a theoretical and methodological basis for practical tools to rapidly assess propellant condition and refine internal ballistics parameters under limited information.

### Keywords

Nitrocellulose propellants, library method, rapid composition verification, inverse identification problems, Amagat's law, Peng-Robinson equation of state.

### 5.1 Introduction

Reliable determination of the composition and energetic characteristics of nitrocellulose propellants remains a critical task for both research applications and practical firing conditions. In real operation, propellant properties evolve due to storage

aging, manufacturing variability, and differences between laboratory and firing environments. As a result, the actual state of a propellant charge may differ substantially from nominal data, which complicates internal ballistics calculations and reduces the reliability of predicted firing parameters. Traditional laboratory methods provide accurate information but are often too slow or technically demanding to support rapid decision-making when only limited experimental data are available.

A key difficulty arises from the inverse nature of the problem: the composition of a propellant must be inferred from indirectly measurable quantities such as combustion temperature, pressure, or gas parameters. These inverse identification problems are typically ill-conditioned, meaning that small measurement uncertainties can lead to significant ambiguities in the reconstructed composition. Direct analytical reconstruction is therefore impractical in many cases, which necessitates alternative computational approaches capable of operating under uncertainty while maintaining sufficient speed for practical use.

This chapter presents a methodology for rapid determination of nitrocellulose propellant composition and condition based on thermodynamic modeling and a library-based computational strategy. The proposed approach separates the process into a preparatory stage, during which a large set of direct thermodynamic problems is solved and structured into a searchable data array, and an operational stage, where experimentally measured parameters are matched with pre-calculated solutions. Such separation allows the main computational burden to be transferred to an offline phase, enabling fast identification procedures under field or laboratory conditions with limited resources.

Particular attention is given to modeling the thermal decomposition of propellants under conditions that differ from conventional laboratory assumptions. These include combustion in closed volumes, the use of real-gas equations of state at elevated pressures, and the possible formation of condensed phases. By combining equilibrium modeling with an efficient encoding and data-reduction procedure, the chapter aims to provide a consistent framework for rapid verification of propellant composition and for improving the accuracy of internal ballistics calculations when only partial experimental information is available.

## **5.2 Condition of the propellant charge**

### **5.2.1 Reasons for the need for rapid determination of propellant condition**

The replenishment rate of propellant stocks depends on production capacity and resources, while storage conditions influence their long-term stability. A distinctive

feature of nitrocellulose (NC) propellants is the gradual change in their chemical composition and performance during storage. Even under controlled conditions, degradation processes cannot be completely prevented. As a result, the characteristics of propelling charges may vary significantly, especially after the expiration of guaranteed storage periods.

Selective batch testing and limited data for individual charges complicate firing planning, since variations in propellant properties affect ballistic performance. During intensive operations, these challenges increase due to the use of charges from different production batches and storage conditions.

These factors highlight the necessity of developing methods for rapid assessment of propellant condition directly at the point of use.

### **5.2.2 Features of the thermal decomposition process of nitrocellulose propellant**

The thermal decomposition of NC propellants strongly depends on environmental conditions. Laboratory studies typically report predominantly gaseous reaction products [1], whereas firing experiments indicate the formation of condensed free carbon, visually observed as soot ejection with propellant gases [2]. The discrepancy is mainly attributed to differences in pressure and temperature during decomposition. According to [2], free carbon formation may occur via carbon monoxide disproportionation (Boudouard-Bell reaction). This effect should be considered when applying laboratory data to internal ballistics modeling.

## **5.3 Determination of the composition of a nitrocellulose propellant charge**

### **5.3.1 Selection of a method for the rapid determination of the composition of nitrocellulose propellant and shot parameters**

Models of internal ballistics processes, as well as of the thermal decomposition of NC propellant under laboratory conditions, are in many cases based on the consideration of equilibrium reactions of propellant gas formation. In such models, the gross formula of the propellant is sufficient for calculations. However, direct experimental determination of gas composition requires complex laboratory techniques.

Gas chromatography is widely used [3], but it has limitations such as long analysis times and sequential determination of components.

New methods, such as Raman spectroscopy, are being studied, but they are still mainly at the laboratory stage and difficult to use in the field [4].

A method was proposed to determine the composition of organic fuel gas from measured combustion data [5]. A similar approach can be used for nitrocellulose propellant.

The following features of the method proposed in [5] should be noted. The model links the composition of the fuel with its combustion products using chemical equilibrium and mass conservation for the main elements (C, H, O, N) [5]. This allows solving the inverse problem of determining the fuel composition from measured data

$$C_{m_c} H_{m_h} O_{m_o} N_{m_n}. \quad (5.1)$$

A list of possible gaseous reaction products is specified, for example



A balance is constructed between the chemical elements in the initial substances (5.1) and the reaction products (5.2). The element balance is formed on the basis of the law of mass action for the equations of formation of the corresponding reaction product components. For example, for  $CO_2$



In addition, mass conservation equations are written for each chemical element from (5.1). Chemical equilibrium constants for gaseous components are most often specified in terms of partial pressures. In this case, it is more rational for the concentrations in the mass action equations to be numerically equal to the partial pressures of the corresponding components. To relate concentrations to partial pressures, the total amount of substance  $M_T$  is introduced. Dalton's law is applied to close the system of equations

$$K_{CO_2}(T) = \frac{P_C \cdot P_O^2}{P_{CO_2}}, \quad (5.4)$$

where  $T$  – the temperature of the mixture of reaction products, determined as a result of the calculations;  $P_C, P_O, P_{CO_2}$  – the partial pressures of the terms in equation (5.3), numerically equal to their concentrations.

On the basis of such a model, the inverse problem can also be solved. The mathematical model determines the interrelation between its parameters. Their assignment as input data or calculation results is subjective in nature. In the example considered above, the following are chosen as input data: the gross formula of the fuel gas in the form

$$C_{b_C} H_{b_H} O_{b_O} N_{b_N}, \quad (5.5)$$

the gross formula of the oxidizer, for example oxygen  $O_2$  or air, the ratio of their volumetric flow rates ( $V_V$ ), and the chemical equilibrium constants for all combustion products  $K_p^i(T)$ . The calculation results are the partial pressures ( $P_i$ ) of the combustion product components (5.2) and their temperature  $T$ .

The unknown coefficients  $b_C$ ,  $b_H$ ,  $b_O$ ,  $b_N$  are treated as additional unknowns, while the measured temperature is input data. Changing  $V_V$  then affects the fuel formula and combustion temperature. Experiments vary input parameters, measure the combustion products, and then use the model to determine the fuel composition. Direct solution can be difficult due to poor conditioning, so the library method is applied [6].

### 5.3.2 Library method for determining the composition of a gaseous fuel

The library method solves direct and inverse problems efficiently through two stages: preparation and solution selection. During preparation, multiple calculations are performed with varied input data to create a library of solutions.

The library is populated by repeatedly solving the direct problem while varying key parameters, including the elemental composition, the volumetric ratio of fuel and oxidizer ( $V_V$ ), and the enthalpy of the combustible gas. Normalization of the elemental composition reduces the number of required solutions without losing information.

During the solution selection stage, input data are matched with stored library entries, and the corresponding solution is selected. This allows rapid determination of firing parameters for specified propellant compositions.

For the inverse problem, the same gas temperature may correspond to different propellant compositions. Measurement errors make this more pronounced, necessitating a specialized algorithm to determine NC propellant composition from technological parameters.

### 5.3.2.1 Procedure for filling the library

When generating the library, a specific feature should be noted. The results of solving the direct problem are transformed into a form suitable for practical use in searching for a solution.

The main portion of the calculated data array obtained from solving the direct problem consists of the partial pressures of gaseous components in the combustion products (CP) mixture. When determining the composition of the initial fuel, these quantities are not directly involved and, therefore, are not included in the generated library.

The fuel composition is formed by varying the parameters  $d_H$ ,  $d_O$ ,  $d_N$ , thus defining a specific elemental composition of the fuel for each realization of the direct problem.

For each such case, the ratio of volumetric flow rates of the fuel and oxidizer,  $V_V$ , is determined.

For all possible combinations of the input parameters  $V_V$ ,  $d_H$ ,  $d_O$ ,  $d_N$ ,  $l_t$  that arise during their variation within specified ranges, an attempt is made to solve the direct problem of determining the combustion products temperature. In some cases, the considered combinations of fuel composition and its enthalpy turn out to be physically incompatible, which makes obtaining a solution impossible. Such calculation variants are excluded from further consideration.

For the remaining successfully implemented variants of the direct problem solution, the set of initial parameters  $d_H$ ,  $d_O$ ,  $d_N$ ,  $l_t$  are encoded as a single numerical identifier based on the positional principle of decimal number representation. Each parameter is normalized within predefined bounds (5.6)

$$\tilde{d}_H = \frac{d_H - d_H^l}{d_H^r - d_H^l} \cdot 100, \quad (5.6)$$

after which the normalized values are encoded into a single positional identifier "E" (Fig. 5.1).

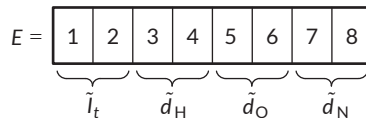


Fig. 5.1 Diagram of positional representation in the form of a single number of normalized values of the original data

As a result, information complexes are formed in which each pair of output parameters of the direct problem solution – the combustion products temperature  $T$  and the volumetric flow rate ratio  $V_V$  – corresponds to a unique number "E" that contains, in a packed form, the values of the input parameters that led to this solution.

At the next stage, the results of calculating the combustion products temperature  $T$  and the volumetric flow rate ratio  $V_V$  are structured into a discretized  $T - V_V$  plane with predefined resolution. The discretization step is selected according to the required computational accuracy and experimental resolution, while cell boundaries are defined by relations (5.7)–(5.9):

$$\Delta T = \frac{T^r - T^l}{N}, \quad \Delta V = \frac{V_V^r - V_V^l}{M}, \quad (5.7)$$

where  $N$  and  $M$  – the numbers of discretization elements (intervals) along the temperature  $T$  axis and the volumetric flow rate ratio  $V_V$  axis, respectively. Cell boundaries on the  $T - V_V$  plane are given by:

$$T_i^l = T^l + \Delta T \cdot (i - 1), \quad T_i^r = T^r + \Delta T \cdot i, \quad i \in [0, N], \quad (5.8)$$

$$(V_V)_j^l = (V_V)^l + \Delta V \cdot (j - 1),$$

$$(V_V)_j^r = (V_V)^r + \Delta V \cdot j, \quad j \in [0, M], \quad (5.9)$$

where  $i$  and  $j$  – the cell indices along the corresponding  $T$  and  $V_V$  axes.

Each cell on the  $T - V_V$  plane is associated with a vector of dimension  $L$  (Fig. 5.2), whose elements are the values of numbers  $E_k$  corresponding to direct problem solutions that fall within this cell. Each cell contains a vector of encoded identifiers  $E_k$  sorted along the enthalpy axis  $I_t$ . The leading digits of  $E_k$  correspond to enthalpy intervals.

Only those  $E_k$  values that fall within the specified enthalpy variation limits are placed into the elements of each vector.

Thus, as a result of preliminary solving a set of direct problems and subsequent processing of the calculated data, a working three-dimensional array is formed. The values contained in this array can be used to determine the composition of various types of fuels, provided that their gross formulas include the chemical elements used in forming the array. The presence of all elements is not mandatory. In particular, the formed array can be used to determine the composition of both oxygen-containing and oxygen-free hydrocarbon fuels when they are combusted either in air or in oxygen without nitrogen admixture.

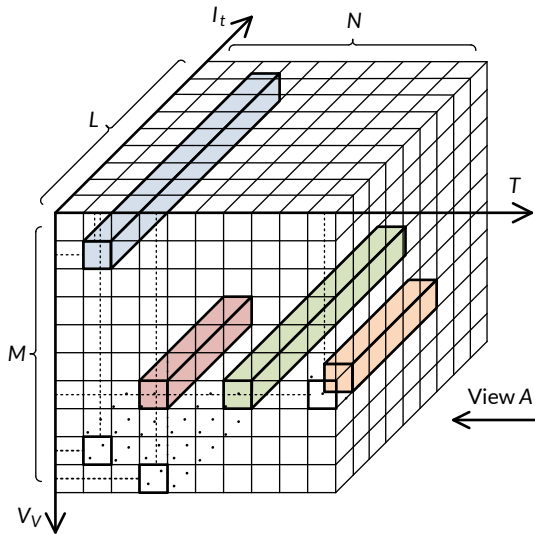


**Fig. 5.2** Scheme of forming a structured working three-dimensional array based on the input data and the results of solving the direct problem

### 5.3.2.2 Determination of fuel composition using library data (inverse problem)

The method for determining the fuel composition using the constructed working three-dimensional array is implemented as a sequential procedure of data selection and reduction, based on matching experimentally measured parameters with the results of a previously solved set of direct problems.

At the first stage, the ratio of volumetric flow rates of oxidizer and fuel ( $V_{v_j}$ ) is varied and fixed. For each prescribed value, the temperature of the combustion products  $T_j$  is measured. The number of variations and corresponding measurements is determined by the number of unknown fuel composition parameters. The unknown parameters of the fuel composition, including elemental amounts and enthalpy, are then narrowed down by selecting library entries consistent with the measurements.

In accordance with the experimentally obtained values  $T_j$  and ( $V_{v_j}$ ), the corresponding cells are selected on the  $T - V_v$  plane of the working three-dimensional array; these cells are shown in **Fig. 5.2** by dashed lines, along with the associated vectors highlighted in color. The data contained in the remaining vectors of the array are

not used at this stage of the analysis. The elements of each selected vector are the numbers  $E_k$ , which encode all possible combinations of the parameters  $d_H$ ,  $d_O$ ,  $d_N$ ,  $I_t$ , that ensure attainment of the measured temperature  $T_j$  at the given volumetric flow ratio corresponding to the selected cell.

At the next step, the selected vectors are projected onto the  $V_V - I_t$  plane (view A in Fig. 5.2), or, in effect, onto the enthalpy axis  $I_t$ . Possible variants of the mutual arrangement of the vector projections are schematically shown in Fig. 5.3 and highlighted in color. Since, for all variations of the volumetric flow ratio, the composition and enthalpy of the fuel being determined remain unknown but invariant, the corresponding values of the numbers  $E_k$  must be present in all considered vectors. On this basis, a subset of elements common to all projected vectors is identified; in Fig. 5.3 this subset is denoted as region  $D$ . Under real conditions, this region may cover more than two discretization intervals along the enthalpy axis. All other vector elements are excluded from further consideration.

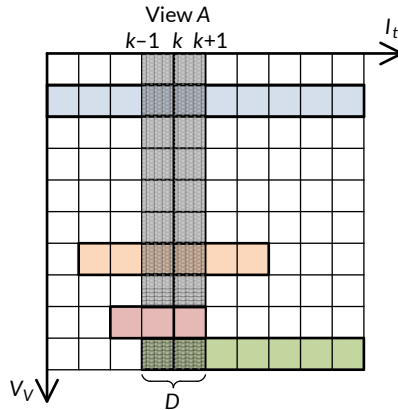


Fig. 5.3 Example of projection of the selected vectors

The most significant digits of  $E_k$  encode the fuel enthalpy. During filtering, encoded numbers are iteratively reordered so that each parameter becomes the leading digit at the corresponding stage (Fig. 5.4), enabling successive reduction of admissible solutions.

The described procedure is successively repeated until all quantities from the list of parameters to be determined –  $d_H$ ,  $d_O$ ,  $d_N$ ,  $I_t$  – have been used. At each subsequent stage, the selection of numbers is performed not by coincidence of enthalpy  $I_t$ , but by the value of the parameter encoded in the most significant digits of the

number  $E_k$  at the current step. Thus, during the second pass this parameter is  $d_H$ , during the third pass it is  $d_O$ , and so on. With each new pass, the number of considered  $E_k$  values decreases.

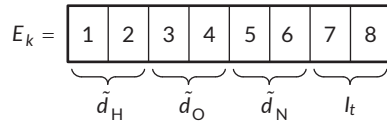


Fig. 5.4 Positional representation scheme in the form of a single number composed of normalized values of the original data after their rearrangement

As a result, a single number  $E_k$  remains, which contains the values of the original parameters in a packed form. These values are consistent with all experimentally measured temperatures  $T_j$  at the specified volumetric flow ratios  $(V_v)_j$ . This number uniquely defines the sought fuel composition and enthalpy.

### 5.3.3 Library method for determining the composition of nitrocellulose propellant

#### 5.3.3.1 Specific features of solving the direct problem when populating the library and determining propellant gas parameters during a shot

The library method is used to solve the inverse problem – determination of the composition of NC propellant. The library is populated based on repeated solutions of the direct problem, i.e., determination of the physical characteristics of propellant gases (PG) under controlled variation of the propellant composition. In the case considered, the physical characteristics of propellant gases during a shot are also determined by solving the direct problem for a previously identified NC propellant composition. In both cases, equilibrium models of propellant gas formation are employed. Under these conditions, the use of identical modeling approaches is considered justified.

Calculation of the propellant gas composition using an equilibrium model that allows for the formation of free carbon predicts its presence. However, laboratory experiments do not confirm this. This does not indicate an error in the equilibrium model but reflects the absence of conditions required for the Boudouard-Bell reaction. To use a single model for solving both the direct and inverse problems, it is sufficient to account for the presence or absence of the possibility of condensed-phase (free carbon) formation.

In the example discussed above, when determining the composition of the combustion products of an organic fuel, only the gaseous phase was considered. In this case, the use of partial pressures is justified. This approach is applied in most calculations of the composition and temperature of propellant gases. However, when the possibility of condensed carbon formation is taken into account, computational difficulties arise in determining its amount via partial pressure. It appears more rational to construct a model using mole fractions of the propellant gas components. This approach allows representation of the composition in both gaseous and condensed phases.

Equilibrium models employ an equation of state (EOS) that defines the relationship between  $p$ ,  $V$ ,  $T$  under thermodynamic equilibrium. The specific form of the EOS depends on the parameter ranges involved. The thermal decomposition of NC propellant is accompanied by high temperatures of 2500–3500 K. At such temperatures and at moderate pressures typical of most laboratory experiments, the ideal gas equation of state is often used, especially at the initial stage of calculations.

At high pressures characteristic of firing conditions, it becomes necessary to account for the finite molecular volume and intermolecular attraction. In this case, a real-gas equation of state is used. Depending on pressure and temperature, ideal-gas, Noble-Abel, virial, and cubic equations of state may be applied. For high-pressure firing conditions, the Peng-Robinson EOS provides the most stable numerical behavior [2].

When increased accuracy is required, more advanced real-gas EOS may be applied; however, for high-pressure firing conditions the Peng-Robinson EOS provides the most stable numerical behavior and is therefore adopted in this work [2]. This property is more important than high accuracy at low pressures.

All numerical calculations were performed using custom-developed software written in C++. The computational experiments included large-scale equilibrium simulations for generating the initial dataset and constructing the solution library. Calculations were carried out on personal computers equipped with Intel Core i5 and i7 processors and 8 GB RAM under Windows 10 OS. Graphical dependencies and diagrams presented in this chapter were prepared using Microsoft Excel.

### 5.3.3.2 Model of the propellant gas formation process using mole fractions

The possibility of the presence of a condensed phase in the composition of propellant gases is not the only reason necessitating the modernization of the model and algorithm described in Section 5.2.2.1 for determining the composition of propellant gases.

In the original model, the pressures of the gaseous reaction products are expressed in pascals (Pa). The chemical equilibrium constants  $K_p$  given in reference literature are defined for such quantities. In the modified model, the quantities of the gaseous components of the propellant gases are expressed in bars (bar). In this case, the partial pressures of the gaseous combustion products are equal to their mole fractions. The amounts of condensed substances can also be expressed in the same units. To write the equations in accordance with the law of mass action, chemical equilibrium constants  $K_X$  defined in terms of mole fractions must be introduced. For a reversible reaction of the form

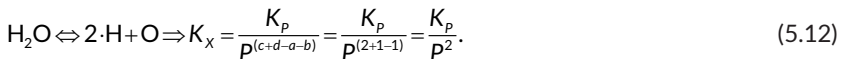


the constants  $K_p$  and  $K_X$  are related by

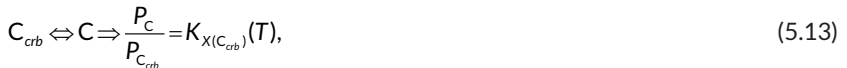
$$K_p = K_X \cdot P^{(c+d-a-b)} \Rightarrow K_X = \frac{K_p}{P^{(c+d-a-b)}}, \quad (5.11)$$

where  $A, B, C, D$  are the chemical species participating in the reaction;  $a, b, c, d$  are the stoichiometric coefficients;  $P$  is the pressure of the mixture of gaseous reaction products expressed in Pa;  $K_p$  is the chemical equilibrium constant defined in terms of partial pressures (a reference value).

For example, for a reaction of the form



A distinctive feature of the model is the introduction of the equation describing soot formation



where  $P_C$  [bar] is the partial pressure and simultaneously the mole fraction of carbon vapor;  $P_{C_{crb}}$  is the mole fraction of the formed soot;  $K_{X(\text{C}_{crb})}(T)$  is the chemical equilibrium constant for the corresponding temperature.

When writing the law of conservation of matter for carbon, the amount of formed soot is taken into account in the balance of propellant combustion products, as in the original version.

The resulting system of equations is nonlinear. The solution is obtained iteratively on the basis of a linearized system of equations. During linearization, it is also necessary to account for the specific features of the mass-action-law equations arising

from the different aggregate states of the propellant gases and soot. In the original model, it was assumed that, at a given temperature, the partial pressure of carbon is independent of the amount of its condensed phase. In this case, when linearizing equation (5.13), the derivative of  $P_C$  was set equal to zero. In the present model, the calculation is performed using mole fractions. In this case, the components  $P_C$  and  $P_{C_{crb}}$  in equation (5.13) have the same status. When linearizing this equation, derivatives are taken with respect to both quantities.

### 5.3.3.3 Influence of experimental conditions on the model of the thermal decomposition process of nitrocellulose propellant

In the original version of the library method [6], the library was populated by modeling the combustion process in an open vessel at constant pressure. The effect of changing the ratio of gaseous fuel and oxidizer on the temperature of the combustion products was used. Due to the constancy of the pressure of the combustion products, as well as the use of the partial pressures of the reaction product components as a measure of their concentration, Dalton's law was used as the closing relation – the pressure in the chamber is equal to the sum of the partial pressures of the reaction products.

When applying the library method to determine the composition of NC propellant, this approach does not correspond to the experimental conditions. Combustion of propellant samples occurs in a closed volume. The pressure of the propellant gases is variable, while their volume is constant. In a closed vessel, varying propellant mass changes afterburning conditions and gas temperature due to oxygen balance effects. When air is used instead of oxygen, nitrogen contained in the air will also act as an inert ballast gas.

At constant vessel volume, instead of the partial pressures of the propellant gas components, their partial volumes are used

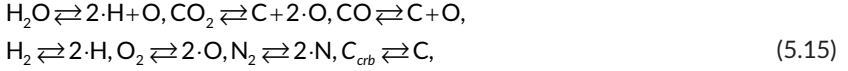
$$V_i = V_{im} \cdot n_i, \quad (5.14)$$

where  $V_{im}$  is the volume of one mole of the corresponding gaseous component of the propellant gases at the temperature and pressure of the gas mixture;  $n_i$  is the number of moles of the corresponding gaseous component of the propellant gas mixture.

The value  $V_{im}$  is determined from the equation of state.

Consider an example of an equilibrium model of thermal decomposition of NC propellant with an overall (gross) formula of the form (5.5), although other chemical

elements may be added if necessary. For the selected reaction products (5.2), with the addition of condensed carbon  $C_{carb}$ , the equations of their formation are written as:



and the chemical equilibrium equations for them are:

$$\begin{aligned} \frac{n_{\text{H}}^2 \cdot n_{\text{O}}}{n_{\text{H}_2\text{O}}} &= K_{n\text{H}_2\text{O}}(T, P), \frac{n_{\text{C}} \cdot n_{\text{O}}^2}{n_{\text{CO}_2}} = K_{n\text{CO}_2}(T, P), \\ \frac{n_{\text{C}} \cdot n_{\text{O}}}{n_{\text{CO}}} &= K_{n\text{CO}}(T, P), \frac{n_{\text{H}}^2}{n_{\text{H}_2}} = K_{n\text{H}_2}(T, P), \\ \frac{n_{\text{O}}^2}{n_{\text{O}_2}} &= K_{n\text{O}_2}(T, P), \frac{n_{\text{N}}^2}{n_{\text{N}_2}} = K_{n\text{N}_2}(T, P), \frac{n_{\text{C}}}{n_{\text{C}_{carb}}} = K_{n\text{C}_{carb}}(T, P). \end{aligned} \quad (5.16)$$

Material balance equations:

$$\begin{aligned} - \text{ for [C]: } m \cdot \frac{b_{\text{C}}}{\mu_{\Sigma}} &= n_{\text{CO}_2} + n_{\text{CO}} + n_{\text{C}} + n_{\text{C}_{carb}}; \\ - \text{ for [H]: } m \cdot \frac{b_{\text{H}}}{\mu_{\Sigma}} &= 2 \cdot n_{\text{H}_2\text{O}} + 2 \cdot n_{\text{H}_2} + n_{\text{H}}; \\ - \text{ for [O]: } 2 \cdot n_{\text{air}} \cdot \varepsilon_{\text{O}_2} + m \cdot \frac{b_{\text{O}}}{\mu_{\Sigma}} &= n_{\text{H}_2\text{O}} + 2 \cdot n_{\text{CO}_2} + n_{\text{CO}} + 2 \cdot n_{\text{O}_2} + n_{\text{O}}; \\ - \text{ for [N]: } 2 \cdot n_{\text{air}} \cdot \varepsilon_{\text{N}_2} + m \cdot \frac{b_{\text{N}}}{\mu_{\Sigma}} &= 2 \cdot n_{\text{N}_2} + n_{\text{N}}, \end{aligned} \quad (5.17)$$

where  $n_{\text{air}}$  is the number of moles of air in the vessel before the start of propellant combustion;  $\varepsilon_{\text{O}_2}, \varepsilon_{\text{N}_2}$  is the fraction of the corresponding gas in air;  $m$  is the mass of propellant subjected to thermal decomposition;  $b_{\text{C}}, b_{\text{H}}, b_{\text{O}}, b_{\text{N}}$  are the numbers of atoms of the corresponding chemical elements in the overall formula of the propellant;  $\mu_{\Sigma}$  is the molecular mass corresponding to the overall formula of the propellant used.

When partial volumes (5.14) are employed in the model under consideration, the closing relation is the equation expressing Amagat's law (fr. *Émile Amagat*). For the adopted list (5.2) of gaseous products of NC propellant thermal decomposition, it has the following form

$$V = n_{\text{H}_2\text{O}} V_{(m)\text{H}_2\text{O}} + n_{\text{CO}_2} V_{(m)\text{CO}_2} + n_{\text{CO}} V_{(m)\text{CO}} + n_{\text{H}_2} V_{(m)\text{H}_2} + n_{\text{O}_2} V_{(m)\text{O}_2} + n_{\text{N}_2} V_{(m)\text{N}_2}. \quad (5.18)$$

In this equation, the terms on the right-hand side correspond to equation (5.14). In the carbon material balance equation (5.17), the term  $n_{c_{cb}}$  is included to account for the presence of condensed carbon. In equation (5.18), the corresponding term is absent. This is due to the small volume of the condensed phase compared to the gaseous phase.

When the numbers of moles  $n_i$  are used as the unknowns, it is necessary to determine the molar chemical equilibrium constants  $K_{n_i}(T,P)$  used in (5.16).

For equations of the form (5.10), the state of chemical equilibrium expressed in terms of molar constants is written as

$$\frac{n_C^c \cdot n_D^d}{n_A^a \cdot n_B^b} = K_n, \quad (5.19)$$

where  $n_C, n_D, n_A, n_B$  are the numbers of moles of the corresponding substances A, B, C, D;  $K_n$  is the chemical equilibrium constant based on the number of moles.

The partial pressures  $p_i$  can be expressed in terms of mole fractions as

$$p_i = X_i \cdot P_\Sigma = \frac{n_i}{\sum n_i} \cdot P_\Sigma, \quad (5.20)$$

where  $X_i$  are the mole fractions;  $P_\Sigma$  is the total pressure of the gas mixture;  $n_i$  is the number of moles of the corresponding substance;  $\sum n_i$  is the total number of moles of the gaseous reaction products.

The chemical equilibrium constants expressed in terms of partial pressures for equations (5.10) have the form

$$K_p = \frac{p_C^c \cdot p_D^d}{p_A^a \cdot p_B^b}, \quad (5.21)$$

where the quantities  $p_i$  are expressed in (bar). For this reason,  $P_\Sigma$  in (5.20) and in the subsequent transformations is also expressed in bar.

As a result, from (5.20) and (5.21) it follows that

$$K_p = \frac{\left(\frac{n_C}{\sum n_i} \cdot P_\Sigma\right)^c \cdot \left(\frac{n_D}{\sum n_i} \cdot P_\Sigma\right)^d}{\left(\frac{n_A}{\sum n_i} \cdot P_\Sigma\right)^a \cdot \left(\frac{n_B}{\sum n_i} \cdot P_\Sigma\right)^b} = \frac{n_C^c \cdot n_D^d}{n_A^a \cdot n_B^b} \cdot \frac{\left(\frac{P_\Sigma}{\sum n_i}\right)^c \cdot \left(\frac{P_\Sigma}{\sum n_i}\right)^d}{\left(\frac{P_\Sigma}{\sum n_i}\right)^a \cdot \left(\frac{P_\Sigma}{\sum n_i}\right)^b} = K_n \cdot \left(\frac{P_\Sigma}{\sum n_i}\right)^{c+d-a-b}. \quad (5.22)$$

From this it follows that

$$K_n(T,P) = K_p(T) \cdot \left( \frac{\sum n_i}{P_\Sigma} \right)^{c+d-a-b}, \quad (5.23)$$

which confirms the dependence of the quantity  $K_n$ , adopted in (5.16), not only on temperature but also on the pressure of the gas mixture. From (5.23), taking into account the equilibrium equation for the condensed phase (5.16), it follows that

$$K_{nU}(T,P) = K_p(T) \cdot \left( \frac{\sum n_i}{P_\Sigma} \right)^{1-1} = K_p(T) \cdot 1 = K_p(T). \quad (5.24)$$

Pressure affects the position of equilibrium for reactions accompanied by a change in the number of moles of gas according to Le Chatelier's principle (fr. *Le Chatelier*). The quantities  $V$  for the corresponding gas and the total pressure  $P_\Sigma$  are related by the real gas equation of state.

#### 5.3.3.4 Effect of pressure magnitude on the composition of propellant gases

In experimental studies, when different amounts of propellant are burned in a closed vessel, the pressure may reach tens of bar. Under firing conditions, this value can reach several thousand bar. A change in pressure leads to a change in the compressibility factor

$$Z = \frac{PV_m}{RT}, \quad (5.25)$$

and, consequently, to a change in the molar concentrations of the gases even when their mass remains constant. Here,  $V_m$  is the molar volume.

Calculated compressibility factors obtained using different equations of state (van der Waals, Noble-Abel, and Peng-Robinson) demonstrate substantial discrepancies over a wide pressure range (Fig. 5.5–5.7). These differences confirm that the choice of equation of state significantly affects the predicted composition of propellant gases and justify the use of the Peng-Robinson EOS for high-pressure conditions.

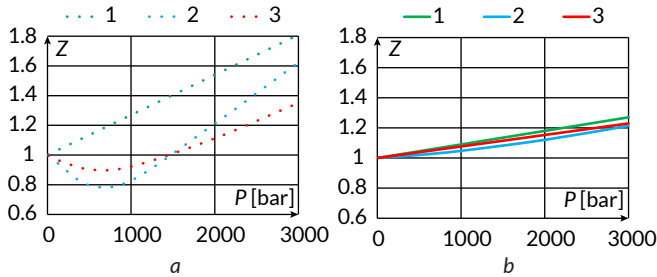


**Fig. 5.5** Compressibility factor  $Z$  as a function of pressure  $P$  for water vapor ( $H_2O$ ):  $a$  - at a temperature of 1000 K;  $b$  - at a temperature of 3000 K; 1 - using the Noble-Abel equation (covolume); 2 - using the van der Waals equation; 3 - using the Peng-Robinson equation

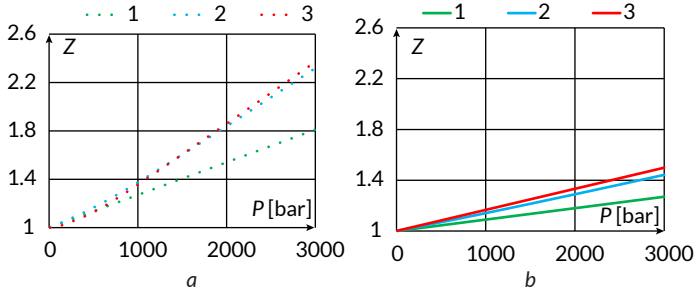


**Fig. 5.6** Compressibility factor  $Z$  as a function of pressure  $P$  for carbon monoxide ( $CO$ ):  $a$  - at a temperature of 1000 K;  $b$  - at a temperature of 3000 K; 1 - using the Noble-Abel equation (covolume); 2 - using the van der Waals equation; 3 - using the Peng-Robinson equation

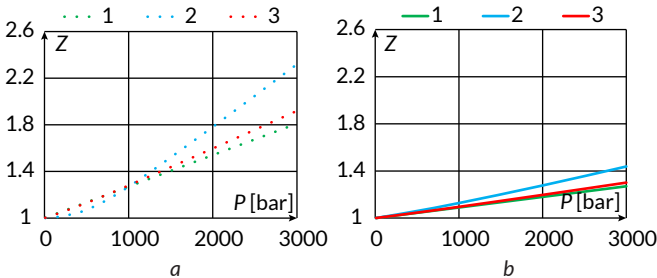


**Fig. 5.7** Compressibility factor  $Z$  as a function of pressure  $P$  for carbon dioxide ( $CO_2$ ):  $a$  - at a temperature of 1000 K;  $b$  - at a temperature of 3000 K; 1 - using the Noble-Abel equation (covolume); 2 - using the van der Waals equation; 3 - using the Peng-Robinson equation

### 5.3.3.5 Effect of pressure on the molar equilibrium constant

In addition to affecting molar concentrations, pressure variations according to relation (5.26) can significantly influence molar equilibrium constants even at nearly constant gas temperature. Within the framework of the mathematical model (5.19)–(5.21), computational studies were carried out on the thermal decomposition process of SB1 propellant [11], characterized by the normalized gross formula  $C_1H_{1.19}N_{0.384}O_{1.45}$  and an enthalpy of formation  $H_f = -96.38$  kJ/mol (normalized per one carbon atom).

Modeling was performed for an evacuated chamber of 0.01 m<sup>3</sup> (10 liters) at propellant masses of 20 and 2400 g, without accounting for condensed carbon formation. The computational case with a mass of 20 g reproduces conditions close to laboratory experiments, while the second corresponds to conditions typical of a firing scenario. The results of the calculations are presented in **Table 5.1**.

**Table 5.1** lists:  $m$  – burned propellant mass;  $K_n$  – molar equilibrium constant;  $n_i/n_\Sigma$  – mole fraction of each component. The last column shows the ratio of the molar equilibrium constants for the experimental and firing conditions. For both propellant masses, the same combustion gas temperature is reached,  $T$  [K] = 2070. When burning  $m = 20$  g of propellant, the pressure in the vessel is  $P = 14.7$  bar. When burning  $m = 2400$  g,  $P = 2530$  bar.

**Table 5.1** Molar equilibrium constants and molar fractions of thermal decomposition products of NC propellant

Component	$m$ [g] = 20		$m$ [g] = 2400		$K_{n20} / K_{n2400}$
	$K_n$	$n_i/n_\Sigma$	$K_n$	$n_i/n_\Sigma$	
CO <sub>2</sub>	4.57E-29	1.19E-01	2.23E-29	9.24E-02	2.05
CO	3.42E-22	4.40E-01	2.38E-22	4.67E-01	1.43
H <sub>2</sub> O	1.04E-14	1.35E-01	5.09E-15	1.59E-01	2.05
NO	6.69E-12	3.92E-10	4.67E-12	5.98E-08	1.43
H <sub>2</sub>	3.63E-07	1.99E-01	2.53E-07	1.73E-01	1.43
O <sub>2</sub>	6.71E-08	1.47E-13	4.69E-08	7.10E-11	1.43
N <sub>2</sub>	3.13E-19	1.08E-01	2.18E-19	1.07E-01	1.43

### 5.3.3.6 Consideration of condensed carbon formation during the thermal decomposition of nitrocellulose propellant

To ensure comparability, database generation and firing simulations must use a unified model. However, a paradoxical situation arises. Equilibrium calculations

that include condensed carbon predict its formation in significant amounts. At the same time, experimental studies of the thermal decomposition of nitrocellulose propellant at low pressure under laboratory conditions do not reveal the formation of free carbon.

On the other hand, in solving internal ballistics problems, the possibility of carbon formation is not taken into account, whereas photographic evidence of firing (Fig. 5.8) demonstrates its limitations. A substantial amount of carbon is formed, and it burns out only during the development of the muzzle flash.



Fig. 5.8 Example of condensed carbon (soot) ejection during firing

In [2], a possible mechanism for the formation of condensed carbon during firing was proposed, and in [9, 10] it was examined with respect to various conditions. Based on model (5.14)–(5.17), calculations were performed to simulate the thermal decomposition process of SB1 propellant [11] in an evacuated vessel with a volume of  $0.01 \text{ m}^3$  (10 liters). Mass fractions of propellant gas components relative to propellant mass are presented in **Table 5.2**. The Peng-Robinson equation of state was used to describe real gas behavior.

Columns 2–3 show mass fractions with and without condensed carbon. These conditions were modeled by the presence or absence of component (5.13) in the model. The comparison confirms the validity of including condensed carbon formation even when it is not observed. The presence of free carbon ( $C_{crb}$ ) is not detected. The data presented in columns 2 and 3 correspond to the pyrolytic phase of the shot (the propellant combustion phase).

Columns 4 and 5 (**Table 5.2**) present data corresponding to the expansion process of propellant gases during the thermodynamic stage of the shot at temperatures  $T = 1000 \text{ K}$  and  $900 \text{ K}$ , respectively. The calculations were performed using the

same model as for the results in column 2. In this case, the formation of free carbon is observed.

**Table 5.2 Mass fractions of propellant gases**

Component	Percentage of gunpowder mass (2400 g)			
	$T [K] = 2070$	$T [K] = 2070$	$T [K] = 1000$	$T [K] = 900$
	$P [\text{bar}] = 2530$	$P [\text{bar}] = 2530$	$P [\text{bar}] = 890$	$P [\text{bar}] = 670$
CO <sub>2</sub>	17.4	17.4	42.3	49.6
CO	56.0	56.0	25.7	11.7
H <sub>2</sub> O	12.3	12.3	11.3	14.4
NO	0.0	0.0	0.0	0.0
H <sub>2</sub>	1.5	1.5	1.6	1.3
O <sub>2</sub>	0.0	0.0	0.0	0.0
N <sub>2</sub>	12.9	12.9	12.9	12.9
C <sub>carb</sub>	0.0	0.0	6.2	10.2

Calculations of the thermal decomposition of SB1 propellant [11] were performed in a sealed vessel with a volume of 0.01 m<sup>3</sup> (10 L) filled with air. The mass of the propellant charge in the calculations varied from 1 to 20 g, which corresponds to the conditions of experimental studies aimed at determining propellant composition using the library method [6]. The modeling results are presented in Fig. 5.9 as dependencies of the number of moles of individual propellant gas components on the mass of the burned propellant. The propellant under consideration is characterized by a negative oxygen balance; as a result, the propellant gases formed during thermal decomposition are incompletely oxidized. Additional oxidation of these products occurs due to the oxygen contained in the air inside the vessel.

For propellant masses up to 6 g, the oxygen in the vessel exceeds the stoichiometric requirement for complete afterburning. In the computational model, the corresponding portion of oxygen is treated as an oxidizer participating in the reactions of complete afterburning, whereas the remaining oxygen, together with the nitrogen of the air, is considered as inert ballast gas. These components are taken into account when determining the thermodynamic parameters of the entire gas mixture, in particular its temperature.

When the propellant mass exceeds 6 g, the oxygen content in the vessel becomes insufficient to ensure complete afterburning of the propellant gases.

The boundary shown in **Fig. 5.9** clearly separates the regions corresponding to excess oxygen ( $m < 6$  g) and oxygen deficiency ( $m > 6$  g), which is of fundamental importance for the interpretation of the modeling results and for the subsequent application of the library method.

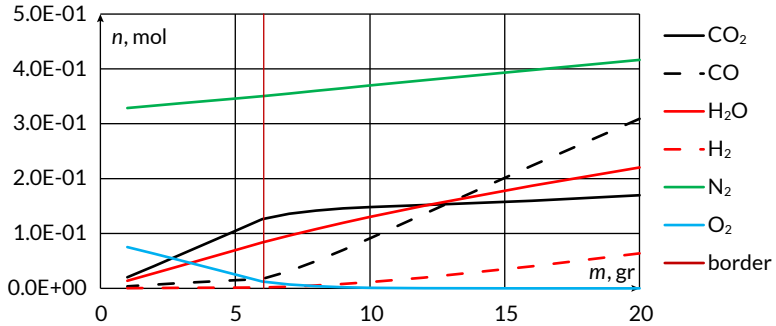


**Fig. 5.9** Number of moles of propellant gas components as a function of the mass of propellant burned in a vessel of volume  $V = 0.01 \text{ m}^3$  filled with air

The limiting value of the propellant mass burned in a vessel of a given volume filled with air is also identified by the nature of the variation of thermodynamic parameters, in particular the temperature, of the propellant gases. The corresponding trends are shown in **Fig. 5.10**, **5.11**.

The obtained data correspond to the conditions of the numerical experiment, the results of which are presented in **Fig. 5.9**. In these plots, as in **Fig. 5.9**, the boundary separating the regions of excess oxygen ( $m < 6$  g) and oxygen deficiency ( $m > 6$  g) is clearly discernible.

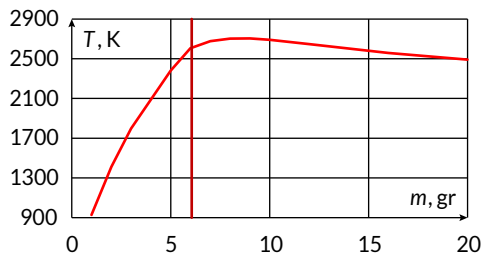


**Fig. 5.10** Variation of the temperature of the propellant gas mixture as a function of the propellant mass burned in a vessel of volume  $V = 0.01 \text{ m}^3$  filled with air

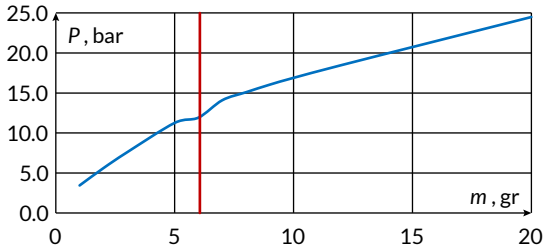


Fig. 5.11 Variation of the pressure of the propellant gas mixture as a function of the propellant mass burned in a vessel of volume  $V = 0.01 \text{ m}^3$  filled with air

## 5.4 Conclusions

The presented material demonstrates that the problem of verifying the composition and energetic characteristics of nitrocellulose propellants under real operating conditions is substantially more complex than assumed within conventional laboratory approaches. The primary reason is the combined effect of storage degradation and differences between laboratory and firing conditions.

The analysis confirms that the use of averaged batch data does not provide the required accuracy for internal ballistics calculations, especially after expiration of the guaranteed storage period or when charges of mixed origin are used. This circumstance substantiates the need to move from selective laboratory control to methods of rapid, in-situ assessment of the current propellant state directly at the point of use.

The differences between laboratory conditions and firing conditions are not only quantitative but also qualitative. In particular, the possible formation of condensed carbon at high pressures and temperatures fundamentally alters the composition of reaction products and the energy balance of the system. Neglecting this effect in internal ballistics models may lead to systematic errors in the estimation of pressure, temperature, and energetic characteristics of propellant gases.

The proposed library method demonstrates its effectiveness as a tool for solving ill-conditioned inverse problems in which a theoretically possible direct analytical reconstruction of propellant composition from measured parameters is practically infeasible. A key advantage of the method is the separation of the computational process into two stages: a resource-intensive preparatory stage for generating the solution library and a fast search stage suitable for operational use. This approach

shifts the main computational burden to the "laboratory" phase and minimizes computational requirements under field conditions.

A distinctive feature of the method is the encoding of composition and enthalpy parameters as numerical identifiers, enabling rapid filtering of admissible solutions even under measurement uncertainty. Adapting the method to closed-volume combustion conditions and employing mole fractions with Amagat's law ensures consistency between laboratory modeling and firing simulations. The Peng-Robinson EOS provides a unified description across the entire pressure range considered.

The obtained results demonstrate that the influence of pressure on the composition of propellant gases at a fixed temperature manifests not only through changes in the compressibility factor and, consequently, molar concentrations, but also through variations in molar equilibrium constants (**Table 5.1**). These constants can vary over a wide range – from approximately 40% to nearly a two-fold change – leading to noticeable changes in mixture composition. For example, the mole fraction of CO<sub>2</sub> may differ by ~22%, H<sub>2</sub>O by ~18%, and H<sub>2</sub> by ~13%. Accounting for this effect explains discrepancies among propellant gas compositions proposed in various empirical models, for which pressure and temperature conditions are often not explicitly specified. The transition from calculations based on partial pressures to those based on molar concentrations made it possible to identify this factor and to justify the use of experimental data obtained at low pressures for firing conditions.

The issue of condensed carbon (soot) formation during the thermal decomposition of nitrocellulose propellants remains debatable only at the level of theoretical models. Experimental observations, including photographic evidence and published studies, unequivocally confirm the practical occurrence of this process. Most internal ballistics calculations focus on the pyrodynamic stage of firing, characterized by high temperatures. Calculations show that, at this stage, conditions for condensed carbon formation are absent, and accounting for or neglecting its formation does not affect the calculated composition of propellant gases.

A different situation arises during the thermodynamic stage of propellant gas expansion, when additional chemical reactions may occur at still high temperatures and pressures. One such reaction is the disproportionation of carbon monoxide (the Boudouard reaction). According to Le Chatelier's principle, increasing pressure shifts the equilibrium of this reaction toward the formation of free carbon. Temperatures on the order of 1000 K and pressures of 30–90 MPa create conditions under which the reaction rate increases by several orders of magnitude compared with normal laboratory conditions. This explains discrepancies between

equilibrium calculations and experimental data and confirms the role of pressure as a key factor in soot formation.

Hydrogen and water vapor in propellant gases further shift the equilibrium, supporting this mechanism. Within the refined model, not only qualitative but also quantitative estimates of condensed carbon formation become possible. Calculations show that during the thermodynamic expansion stage its amount may reach 10–16% of the propellant mass, in good agreement with literature data.

The proposed model enables calculation of the composition and parameters of nitrocellulose propellant thermal decomposition products at moderate pressures, thereby allowing the formation of a library of calculated data. Using this library to determine propellant composition requires variation of propellant gas afterburning conditions, including preliminary filling of the experimental vessel with air or other oxygen-containing mixtures.

### **Conflict of interest**

The authors declare that they have no conflict of interest in relation to this research, whether financial, personal, authorship or otherwise, that could affect the research and its results presented in this paper.

### **Use of artificial intelligence statement**

The authors confirm that they did not use artificial intelligence technologies when creating the current work.

### **Authors' contributions**

**Oleksandr Brunetkin:** Conceptualization, Methodology, Development of library-based verification method, Supervision, Writing – original draft.

**Oksana Maksymova:** Thermochemical modeling, Data analysis, Numerical simulations, Visualization.

**Yevhenii Dobrynin:** Formal analysis, Validation of computational models, Interpretation of results, Writing – review & editing.

**Oleksandr Sidelnykov:** Literature review, Data curation, Comparative analysis, Writing – review & editing.

## References

1. Boltenkov, V., Brunetkin, O., Dobrynin, Y., Maksymova, O., Kuzmenko, V., Gultsov, P. et al. (2021). Devising a method for improving the efficiency of artillery shooting based on the Markov model. *Eastern-European Journal of Enterprise Technologies*, 6 (3 (114)), 6–17. <https://doi.org/10.15587/1729-4061.2021.245854>
2. Dobrynin, Y., Volkov, V., Maksymov, M., Boltenkov, V. (2020). Development of physical models for the formation of acoustic waves at artillery shots and study of the possibility of separate registration of waves of various types. *Eastern-European Journal of Enterprise Technologies*, 4 (5 (106)), 6–15. <https://doi.org/10.15587/1729-4061.2020.209847>
3. Dobrynin, Y., Brunetkin, O., Maksymov, M., Maksymov, O. (2020). Constructing a method for solving the riccati equations to describe objects parameters in an analytical form. *Eastern-European Journal of Enterprise Technologies*, 3 (4 (105)), 20–26. <https://doi.org/10.15587/1729-4061.2020.205107>
4. Brunetkin, O., Beglov, K., Brunetkin, V., Maksymov, O., Maksymova, O., Haval-iukh, O., Demydenko, V. (2020). Construction of a method for representing an approximation model of an object as a set of linear differential models. *Eastern-European Journal of Enterprise Technologies*, 6 (2 (108)), 66–73. <https://doi.org/10.15587/1729-4061.2020.220326>
5. Brunetkin, O., Maksymov, M., Brunetkin, V., Maksymov, O., Dobrynin, Y., Kuzmenko, V., Gultsov, P. (2021). Development of the model and the method for determining the influence of the temperature of gunpowder gases in the gun barrel for explaining visualize of free carbon at shot. *Eastern-European Journal of Enterprise Technologies*, 4 (1 (112)), 41–53. <https://doi.org/10.15587/1729-4061.2021.239150>
6. Brunetkin, O., Maksymov, M., Dobrynin, Y., Demydenko, V., Sidelnykov, O. (2024). Development of a process model for determining the composition and energy characteristics of a pyrotechnic mixture using the library method. *EUREKA: Physics and Engineering*, 5, 99–112. <https://doi.org/10.21303/2461-4262.2024.003453>
7. Brunetkin, O., Dobrynin, Y., Maksymenko, A., Maksymova, O., Alyokhina, S. (2020). Inverse problem of the composition determination of combustion products for gaseous hydrocarbon fuel. *Computational Thermal Sciences: An International Journal*, 12 (6), 477–489. <https://doi.org/10.1615/computthermalscien.2020034878>
8. Maksymov, M. V., Brunetkin, O. I., Beglov, K. V., Alyokhina, S. V., Butenko, O. V. (2022). Automatic Control for the Slow Pyrolysis of Organic Materials with

- Variable Composition. *Advanced Control Systems*. River Publishers, 397–434. <https://doi.org/10.1201/9781003337010-16>
9. Brunetkin, O., Beglov, K., Maksimov, M., Ulitskaja, E. (2023). Model and method of controlled pyrolysis of organic sub-stances of variable composition. *International Scientific Technical Journal "Problems of Control and Informatics"*, 66 (1), 134–146. <https://doi.org/10.34229/1028-0979-2021-1-12>
  10. Brunetkin, O., Sidelnikov, O., Maksymov, M., Dobrynin, Y. (2025). Improving the model for determining the composition of gunpowder gases during thermal destruction of gunpowder in a limited volume space. *Eastern-European Journal of Enterprise Technologies*, 3 (6 (135)), 35–45. <https://doi.org/10.15587/1729-4061.2025.330654>
  11. Dobrynin, Y., Maksymov, M., Boltenkov, V. (2020). Development of a method for determining the wear of artillery barrels by acoustic fields of shots. *Eastern-European Journal of Enterprise Technologies*, 3 (5 (105)), 6–18. <https://doi.org/10.15587/1729-4061.2020.206114>
  12. Dobrynin, Y. V., Boltenkov, V. O., Maksymov, M. V. (2020). Information technology for automated assessment of the artillery barrels wear based on SVM classifier. *Applied Aspects of Information Technology*, 3 (3), 117–132. <https://doi.org/10.15276/aait.03.2020.1>
  13. Suykens, J. A. K., Van Gestel, T., De Brabanter, J., De Moor, B., Vandewalle, J. (2002). *Least Squares Support Vector Machines*. Singapore: World Scientific, 295.
  14. Xia, X.-L., Jiao, W., Li, K., Irwin, G. (2013). A Novel Sparse Least Squares Support Vector Machines. *Mathematical Problems in Engineering*, 2013, 1–10. <https://doi.org/10.1155/2013/602341>
  15. LS-SVMlab toolbox. Available at: <https://www.esat.kuleuven.be/sista/lssvmlab/>
  16. James, G., Witten, D., Hastie, T., Tibshirani, R. (2013). *Support Vector Machines. An Introduction to Statistical Learning*. Springer Texts in Statistics, Vol. 103. New York: Springer, 337–372. [https://doi.org/10.1007/978-1-4614-7138-7\\_9](https://doi.org/10.1007/978-1-4614-7138-7_9)